Section A -Research paper

Wear Behavior of PMMA-Based Polymer Composite

Deore Harshal,
Affiliation: SNJB's Late Sau.K.B.Jain College of Engineering Chandwad,
deore.hscoe@snjb.org
N. Ramanan,
Affiliation: Sri Jayaram institute of engineering and technology gummudipundi Chennai,
ramananinjs2020@gmail.com
Sancheti Santosh
Affiliation: SNJB's Late Sau.K.B.Jain College of Engineering Chandwad,
santusancheti@gmail.com
doi: 10.48047/ecb/2023.12.si4.891

Abstract: In recent years, manufacturing industries have faced intense competition due to globalization. Companies have adopted various management philosophies to achieve greater success while emphasizing material properties for industrial component production. The automotive industry, in particular, requires strong and lightweight materials. Polymer matrix composites (PMCs) have emerged as a vital solution.

PMCs consist of an organic polymer matrix binding various short or continuous fibers. They are designed to distribute loads between fibers through the matrix, providing several benefits, including outstanding strength in the direction of reinforcements, high stiffness, and light weight. Additional benefits include excellent abrasion and corrosion resistance.

The purpose of this article is to identify the ideal wear testing parameters for PMCs. The composite materials studied were fabricated using polymethyl methacrylate (PMMA) and 5% nano B4C through injection molding. In order to determine the most effective parameters, the article concentrates on determining the friction rate and coefficient. The findings of this study can be applied to the wear area of automotive components.

Keyword: PMMA, Wear Analysis, Grey relation analysis is performed, Design of Experiments

1. Introduction

The study analyzed the wear performance of PMMA composites filled with ZrO2. Wear test results at room temperature indicated that increasing the ZrO2 weight fraction to 30% resulted in smoother worn surfaces. Another study examined the tribological characteristics of nano-reinforced PMMA composites made by ultrasonic dispersion and cold casting. Results indicated that as time and the ratio of TiO2-ZnO grew, wear and friction coefficients decreased.

To test graphite-filled SiO2-PMMA composites, silane surface treatment was used. Analysis using Fourier Transform Infrared Spectroscopy demonstrated that the presence of active groups enhanced the polarity of SiO2, thus enhancing bond properties and sample hardness. The

research showed that employing nano-SiO2 and TiO2 particles to reinforce PMMA composites resulted in noticeable strengthening effects, with wear mechanisms switching from micro-cutting, multi-plastic deformation, and adhesive wear to abrasive and abrasive and brittle fracture wear.

The tribological behavior of silicone substrate-coated PMMA against perfluoro decyl trichlorosilane was studied. The results indicated that the viscoelastic behaviour of PMMA was followed by the friction coefficient vs. applied-temperature curves, pointing to molecular relaxation of PMMA as the key factor. In comparison to unfilled composites, treated and untreated nano-ZnO reinforced hybrid glass/PTFE fabric composites showed enhanced wear resistance and friction reduction.

Smaller particles were shown to be more efficient in lowering wear rate and friction coefficient than bigger particles during dry sliding tests on nanocomposite samples on a steel counter face. The inclusion of nanoparticles might frequently boost wear resistance and decrease the average coefficient of friction, according to a study on poly(ethylene terephthalate) (PET) filled with alumina nanoparticles and dry slid against a steel counter face.

Under dry sliding circumstances, the tribological characteristics of high-temperature-resistant thermoplastic composites, such as polyetheretherketone (PEEK) and polyetherimide (PEI), reinforced with short carbon fibre (SCF), graphite flakes, and sub-micro particles of TiO2 and ZnS, were studied. The wear resistance and load-carrying capacity of basic polymers were significantly improved by conventional fillers like SCF and graphite flakes.

Carbon fibre (CF) surfaces were modified using the titanium dioxide (TiO2) surface functionalization method. Due to CF's strong impact strength, the izod impact strength of CF/HDPE composites increased with CF content. Contrarily, the addition of TiO2 raised the impact strength of the composites even more, most likely as a result of the reinforcement action of TiO2.

Numerous fillers, such as short carbon fibre (CF), graphite, polytetrafluoroethylene (PTFE), and nano-TiO2, were used to increase the wear resistance of epoxy. Combining nano-TiO2 with traditional fillers resulted in the composition with the best wear resistance. Nanoscale rolling effects of nanoparticles greatly improved wear resistance by shielding composite surfaces from more severe wear processes, according to SEM and AFM worn surface investigations of nanocomposites.

Investigated were the effects of coupling agent, coupling agent followed by HNO3 on PTFE with carbon nanofiber (CNF). The best anti-wear property was obtained by treating CNF with HNO3 first, then treating it with a coupling agent. This resulted to a wear rate that was 30% lower than untreated CNF-filled PTFE under a 200N load. According to SEM tests, surface modification, notably with HNO3, followed by coupling agent treatment, increased CNF dispersion in PTFE composites and decreased the abrasive wear of CNF/PTFE composites.

A microhardness tester and a pin-on-disc wear device were used to measure the effects of these particles on microhardness, friction, and dry sliding wear behaviour. According to experimental results, BMI's specific wear rate and friction coefficient may both be reduced at comparatively

low concentrations of nano-ZrO2. Another research looked at the specific wear rate of jute-reinforced epoxy composites with different fibre weight percentages (10, 20, 30, and 40 wt%) and different chemical treatments (alkaline and benzoyl chloride). According to the study, the specific wear rate of jute epoxy composites decreased as sliding distance rose while increasing as average load increased. In a steady-state setting, samples with a 30 weight percent fibre loading showed the lowest specific wear rate at varied sliding distances and under typical loading circumstances. Comparing benzoyl chloride-treated composites to untreated and alkali-treated composites, the former showed greater abrasive wear resistance.

Unidirectional fiber-reinforced polymer composites' abrasive wear was predicted using a model. The proposed model is cyclical (or quasi-steady-state), in contrast to steady-state wear, when various components wear at the same pace. In this model, the fibre and matrix do not always wear at the same rate.

2. Wear analysis

Wear is the process of material loss from either one or both solid surfaces. Instead of adopting wear-resistant alloys, as wear mostly affects exterior surfaces, it is more practical and cost-effective to change the surfaces of current metals. Using a pin-on-disc testing device, several materials were examined for dry sliding wear. A dead weight loading mechanism provided pressure to the pin by pressing it against the counter face of a revolving disc.

Under standard loads of 5N, 10N, and 15N with sliding velocities of 1m/s, 2m/s, and 3m/s, all samples were put through wear testing. The tests covered total sliding distances of approximately 500m, 750m, and 1000m. The pin specimens measured 30mm in length and had a cross-sectional area of 10x10 mm. Figure 1 illustrates the specimens used for wear testing.

Figure1: Specimens for Wear Test

To make sure the steel disc made contact with a clean, flat surface before testing, the pin sample surfaces were polished with 80-grit emery paper. Before and after each test, the samples and wear track were cleaned with acetone and weighed with a microbalance (accurate to 0.0001 grammes). By measuring wear volume loss per unit of sliding distance, the height loss approach

calculated the wear rate. In the experiment, variables including weight, speed, and distance were taken into account.

To evaluate tribology, the pin-on-disc test was used. Three steps of the testing process were involved:

1. To support the load over its whole cross-section, the pin surface was first flattened. Before testing, the pin sample was polished with 80-grit emery paper to accomplish this.
2. Run-in-wear, the second step, reduced the turbulence that initially accompanied friction and wear curves.
3. The material transfer processes (material transfer from the pin to the disc, wear debris production, and subsequent removal) interacted dynamically in the third and final stage, known as constant or steady-state wear.

Cotton soaked in ethanol was used to clean the pin and disc prior to testing. Pin-on-disc technology is shown in Figure 2.

Figure2: Pin on Disc Apparatus

Figure 2: shown in a pin on disc apparatus. the apparatus is Manufactured by DUCOM Instrument. the Disc diameter is 160mm, and the disc's thickness is 12mm. The instrument used a find out the wear rate of the samples

3. Design of experiments

Using design of experiments (DOE) methodologies, designers may analyse the simultaneous individual and interaction impacts of a wide range of variables that may influence the output outcomes of any design. Process parameters including load, sliding speed, and sliding distance have been examined using the Taguchi L27 orthogonal array. Table 1 displays the design of the experiments for the wear rate and friction coefficient.

Table 1. Design of Experiments for Wear Rate and Coefficient of friction

Ex.No.	Load (N)	Sliding Speed (mm/s)	Sliding Distance (mm)
1	5	1	500
2	5	1	750
3	5	1	1000
4	5	2	500
5	5	2	750
6	5	2	1000
7	5	3	500
8	5	3	750
9	5	3	1000
10	10	1	500
11	10	1	750
12	10	1	1000
13	10	2	500
14	10	2	750
15	10	2	1000
16	10	3	500
17	10	3	750
18	10	3	1000
19	15	1	500
20	15	1	750
21	15	1	1000
22	15	2	500
23	15	2	750
24	15	2	1000
25	15	3	500
26	15	3	750
27	15	3	1000

Table 1 shows that the table was explained the Design of Experiments

4. Material Removal Rate

The same procedure is followed as the wear for calculating the material removal rate.

Table 2. Signal/Noise ratio values for the original response data (experimental results)

Ex.No.	Load (N)	SS (mm/s)	SD (mm)	MRR	Dimensional Error
1	5	1	500	0.1329	3.26
2	5	1	750	0.105375	3.39

3	5	1	1000	0.103125	3.50
4	5	2	500	0.126075	3.87
5	5	2	750	0.1122	3.87
6	5	2	1000	0.1071	3.98
7	5	3	500	0.107625	4.10
8	5	3	750	0.1047	4.15
9	5	3	1000	0.099975	4.19
10	10	1	500	0.1623	4.21
11	10	1	750	0.14415	4.24
12	10	1	1000	0.127425	4.24
13	10	2	500	0.157875	4.28
14	10	2	750	0.14385	4.33
15	10	2	1000	0.138	4.38
16	10	3	500	0.174525	4.42
17	10	3	750	0.1449	4.47
18	10	3	1000	0.144225	4.52
19	15	1	500	0.21075	4.52
20	15	1	750	0.17955	4.56
21	15	1	1000	0.154575	4.61
22	15	2	500	0.225225	4.65
23	15	2	750	0.20355	4.70
24	15	2	1000	0.178125	4.75
25	15	3	500	0.22035	4.79
26	15	3	750	0.2073	4.84
27	15	3	1000	0.188325	4.88

Table3. Normalized S/N ratio values
(output response data after data pre-processing)

Ex.No.	Norm MRR	Norm DE	Abs MRR	Abs DE
1	0.262874	1	0.8671	0.737126
2	0.043114	0.918519	0.894625	0.956886
3	0.02515	0.853704	0.896875	0.97485
4	0.208383	0.625309	0.873925	0.791617
5	0.097605	0.624691	0.8878	0.902395
6	0.056886	0.553086	0.8929	0.943114
7	0.061078	0.481379	0.892375	0.938922
8	0.037725	0.452922	0.8953	0.962275

9	1.11E-16	0.424465	0.900025	1
10	0.497605	0.416049	0.8377	0.502395
11	0.352695	0.397531	0.85585	0.647305
12	0.219162	0.396008	0.872575	0.780838
13	0.462275	0.367551	0.842125	0.537725
14	0.350299	0.339095	0.85615	0.649701
15	0.303593	0.310638	0.862	0.696407
16	0.59521	0.282181	0.825475	0.40479
17	0.358683	0.253724	0.8551	0.641317
18	0.353293	0.225267	0.855775	0.646707
19	0.884431	0.224074	0.78925	0.115569
20	0.635329	0.196811	0.82045	0.364671
21	0.435928	0.168354	0.845425	0.564072
22	1	0.139897	0.774775	0
23	0.826946	0.11144	0.79645	0.173054
24	0.623952	0.082984	0.821875	0.376048
25	0.961078	0.054527	0.77965	0.038922
26	0.856886	0.02607	0.7927	0.143114
27	0.705389	-0.00239	0.811675	0.294611

Table4. Grey Relational Coefficient values and the Grey Relational Grade

GRC MRR	GRC DE	GRG
0.365738	0.404163	0.38495
0.358519	0.343198	0.350859
0.357942	0.339017	0.34848
0.363921	0.387112	0.375516
0.360282	0.356533	0.358408
0.358963	0.346473	0.352718
0.359099	0.347482	0.35329
0.358346	0.341933	0.350139
0.357136	0.333333	0.345235
0.373776	0.498805	0.436291
0.368772	0.435804	0.402288
0.364279	0.390369	0.377324
0.372544	0.481823	0.427183
0.368691	0.434896	0.401793
0.367107	0.417918	0.392513

0.377223	0.552614	0.464919
0.368976	0.43809	0.403533
0.368793	0.436031	0.402412
0.387822	0.812257	0.60004
0.378659	0.578255	0.478457
0.37163	0.469893	0.420761
0.392226	1	0.696113
0.385669	0.742883	0.564276
0.378251	0.570745	0.474498
0.390732	0.927778	0.659255
0.386787	0.777467	0.582127
0.381192	0.629239	0.505215

5. Analysis of Variance (ANOVA)

Better if it's bigger When the original sequence's goal value is infinite, this condition is applied. When the response is to be maximised, the following equation is utilised.

$$\square = -10 \times \square\square\square_{10}\left(\frac{1}{\square}\sum \quad \frac{1}{\square^2_{\square}}\right) \qquad (1)$$

Table 5. ANOVA FOR MRR

Source	DF	Seq SS	Adj SS	MS	F	P
Pressure	1	0.032826	2.6E-06	2.6E-06	0.088	0.769722
SoD	1	0.000286	0.000251	0.000251	8.651	0.009128
TS	1	0.004255	3.01E-05	3.01E-05	1.039	0.322357
P*P	1	0.000158	0.000158	0.000158	5.45	0.032092
SoD*SoD	1	9.58E-05	9.58E-05	9.58E-05	3.308	0.086621
TS*TS	1	0.000084	0.000084	0.000084	2.9	0.106779
P*SoD	1	0.000837	0.000837	0.000837	28.887	0.00005
P*TS	1	0.000519	0.000519	0.000519	17.911	0.000561
TS*SoD	1	0.000216	0.000216	0.000216	7.44	0.014326
Error	17	0.000492	0.000492	0.000029		
Total	26	0.039768				

MRR = 0.277979 - 0.000488646 Pressure - 0.0590906 SoD - 0.000407188 TS + 1.28229e-005 P*P - 0.00399583 SoD*SoD + 5.84635e-007 TS*TS + 0.0004175

P*SoD - 4.10937e-006 P*TS + 5.29688e-005 TS*SoD

Summary of Model

S = 0.00538177 R-Sq = 98.76% R-Sq(adj) = 98.11%

R-Sq(pred) = 96.96%

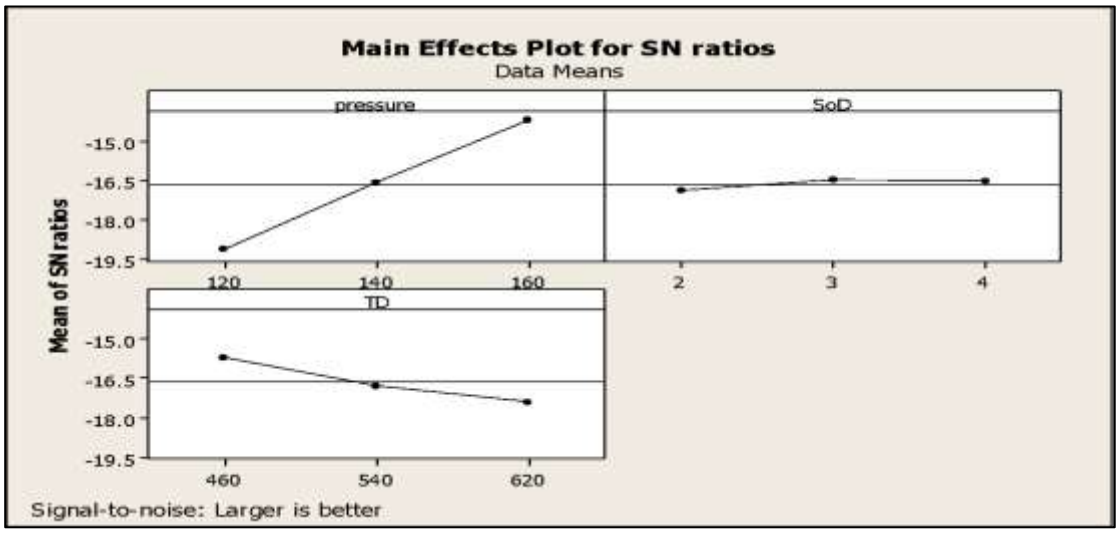

Figure 3 Signal to Noise Ratios(MRR)

From figure 3 it is observed that Pressure of 140 N, sliding speed of 750mm/sec and SOD of 3 mm gives optimal wear behaviour.

Table 6. ANOVA For GRG

Source	DF	Seq SS	Adj SS	MS	F	P
P	1	0.172313	0.00255	0.00255	5.979	0.025663
SoD	1	0.003951	0.00079	0.00079	1.8534	0.191165
TS	1	0.033662	0.000083	8.25E-05	0.1936	0.665518
P*P	1	0.011377	0.011377	0.011377	26.6799	0.000078
SoD*SoD	1	0.0009	0.0009	0.0009	2.1106	0.16449
TS*TS	1	0.001005	0.001005	0.001005	2.3566	0.143156
P*SoD	1	0.006672	0.006672	0.006672	15.6466	0.001021
P*TS	1	0.019814	0.019814	0.019814	46.4623	0.000003
TS*SoD	1	0.000209	0.000209	0.000209	0.4908	0.493066
Error	17	0.00725	0.00725	0.000426		
Total	26	0.257153				

GRG = 1.2471 - 0.0154131 P - 0.104949 SoD + 0.000674381 TS + 0.000108865 P*P - 0.0122478 SoD*SoD + 2.02216e-006 TS*TS + 0.00117901 P*SoD - 2.53963e-005 P*TS + 5.22016e-005 TS*SoD

Summary of Model

S = 0.0206505 R-Sq = 97.18% R-Sq(adj) = 95.69%

R-Sq(pred) = 93.52%

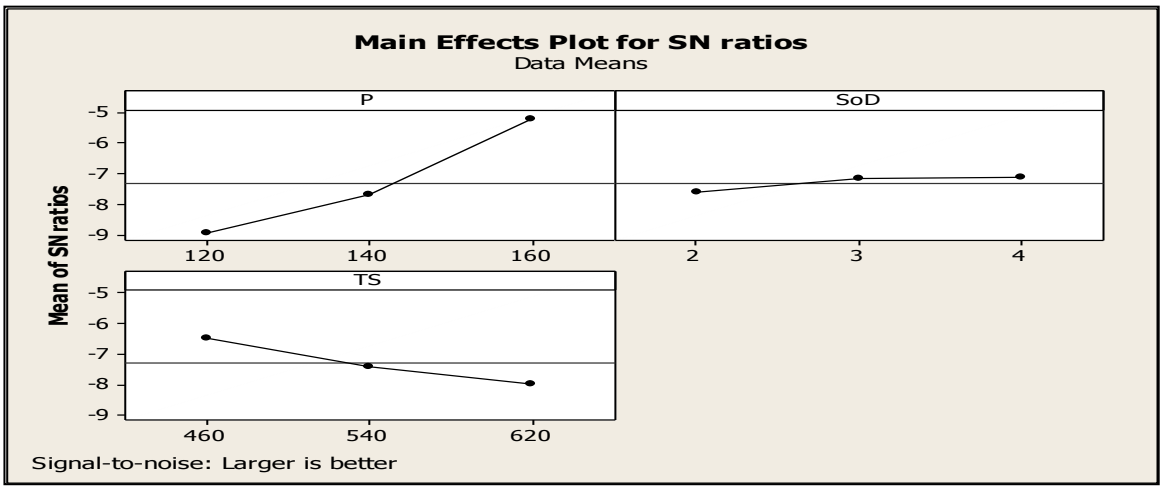

Figure 4 Signal to Noise Ratios Grey Relational Grade (GRG)

From figure 4 it is observed that load of 140 N, sliding speed of 540mm/sec and SOD of 3 mm gives optimal wear behavior

Table 7. ANNOVA for Dimensional Error

Source	DF	Seq SS	Adj SS	MS	F	P
P	1	3.54697	0.12004	0.120044	17.1858	0.000677
SoD	1	0.82095	0.133	0.133	19.0406	0.000423
TS	1	0.04885	0.00045	0.000451	0.0646	0.802422
P*P	1	0.04477	0.04477	0.044767	6.4089	0.021509
SoD*SoD	1	0.01028	0.01028	0.010275	1.4711	0.241763
TS*TS	1	0.00007	0.00007	0.000072	0.0103	0.920261
P*SoD	1	0.1781	0.1781	0.178104	25.4978	0.000099
P*TS	1	0.00245	0.00245	0.002452	0.351	0.561329
TS*So	1	0.0005	0.0005	0.00057	0.0825	0.77747

D		8	8	6		3
Error	17	0.11875	0.11875	0.006985		
Total	26	4.77176				

DE = -7.55335 + 0.105758 P + 1.36142 SoD + 0.00157676 TS - 0.000215944 P*P - 0.0413833 SoD*SoD + 5.41667e-007 TS*TS - 0.00609139 P*SoD - 8.93403e-006 P*TS - 8.65972e-005 TS*SoD

Summary of Model

S = 0.0835767 R-Sq = 97.51% R-Sq(adj) = 96.19%

R-Sq(pred) = 93.40%

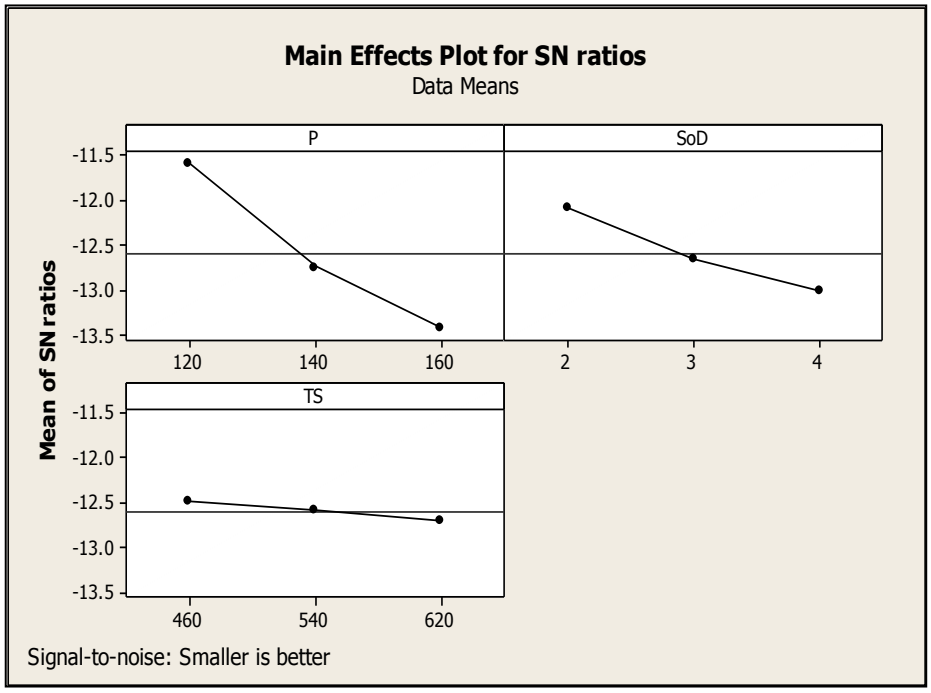

Fig 5:Signal to S Ratio

From figure 5 it is observed that load of 140 N, sliding speed of 540mm/sec and SOD of 3 mm gives optimal wear behavior

6. Grey Relational Analysis (GRA)

Cutting speed, feed, and tool diameter—all regarded to be process parameters—have been examined using the Taguchi L27 orthogonal array, together with fuzzy logic and grey relations. The complicated relationships between the various response properties were optimised using

GRA. The experiment design for wear rate and coefficient of friction is displayed in Table 2. As is clear, it is quite challenging to optimise the multiple output response. Effectively measuring the values between the sequences (or, more specifically, the data difference values between sequences), is helpful. The 27 trials performed in accordance with Taguchi's orthogonal array will be regarded as 27 subsystems for GRA. 27 subsystems' effects on the response variable are examined by the GRA. There were 27 tests for the machining of composite materials, each of which took into account a comparable sequence. In the experiment, the lowest values of tangential force, thrust force, and torque were produced by the GRG (grey relational grade) with the highest weight. As a result, the grey relational analysis approach was used to derive the single goal optimisation from the multi-objective issue. The following procedures were used in

6.1.GRA Procedure

Step 1: The experimental results' initial response data was converted into a Signal-to-Noise ratio (S/N) ratio (η).

One of the greatest strategies for the design of experiments has long been the Taguchi method. The Taguchi method's S/N ratio was utilised to determine the response parameters. The study calculates the S/N ratio for each control factor. As a result, the noises indicate deviations from the average replies, and the signals serve as indications to determine the average responses. S/N ratios are divided into three types: nominal, bigger, and smaller. The lesser the S/N ratio, the better. The significance of categories is highlighted in the next paragraph.

(a) The following equation will be used to normalise the original sequence if lower the better is taken into consideration. Smaller the better,

$$\eta = -10 \times \log_{10}\left(\frac{1}{n}\sum y_i^2\right) \quad (2)$$

(b) The bigger, the better When the goal value of the original sequence is infinite, this condition is utilised. When maximising the response, the following equation is utilised.

$$\eta = -10 \times \log_{10}\left(\frac{1}{n}\sum \frac{1}{y_i^2}\right) \quad (3)$$

(c) Nominal the best: The following equation is used to target a response. (Best nominally)

$$\eta = 10 * \log_{10}(\mu^2/\sigma^2) \quad (4)$$

where n is the experiment's repeat count, yi denotes the average measured value of experimental data i, and μ2 denotes the mean of the observed data;

σ2– variation in the measured data. The smaller the better characteristic for torque, thrust, and tangential force. Consequently, Equation 1 is used to determine the loss function. The experimental findings' signal-to-noise ratios (original response data) are shown in Table 2.

Table 8: Design of Experimentation with L27 orthogonal array and experimental results

Ex.No.	Load (N)	SlidingSpeed (rpm)	Sliding Distance(mm)
1	5	1	500
2	5	1	750
3	5	1	1000
4	5	2	500
5	5	2	750
6	5	2	1000
7	5	3	500
8	5	3	750
9	5	3	1000
10	10	1	500
11	10	1	750
12	10	1	1000
13	10	2	500
14	10	2	750
15	10	2	1000
16	10	3	500
17	10	3	750
18	10	3	1000
19	15	1	500
20	15	1	750
21	15	1	1000
22	15	2	500
23	15	2	750
24	15	2	1000
25	15	3	500
26	15	3	750
27	15	3	1000

Step 2: Normalization of S/N ratio values (Data Pre-processing)

The S/N ratio is normalised in order to prepare the raw data for the analysis, and this process is regarded as the first stage in GRA. Here, a similar sequence is produced as a result of the original sequence being transformed. Since the range and data vary from one sequence to another, linear normalization—often referred to as data pre-processing—is utilised. When the sequence's dispersion range is quite wide, this is also considered required. Only the range of the S/N ratio's linear normalisation fluctuates between zero and one. The values produced using the following formulas are shown in Table 6.9 along with the normalised values.

Normalize yij as zij.

For smaller the better values,

$$\square_{\square\square} = \frac{[(\square_{\square\square}) - (\square_{\square\square})]}{[(\square_{\square\square}) - \square\square\square(\square_{\square\square})]} \qquad (.5)$$

For larger the better values,

$$\square_{\square\square} = \frac{[(\square_{\square\square}) - \square\square\square(\square_{\square\square})]}{[(\square_{\square\square}) - \square\square\square(\square_{\square\square})]} \qquad (6)$$

where yij is the data that correspond to the signal to noise ratio values reported in Table 2; zij is the normalised value for the ith experiment/trial for the jth-dependent variable/ reaction. The corresponding maximum and minimum S/N ratio values are max(yij) and min(yij) in Equations 4 and 5 above.

Step 3: From the normalised S/N ratio result, the Grey Relational Coefficient (GRC) should be calculated.The grey relational analysis is used to gauge how connected the two systems are to one another. GRC is used to compare the optimal S/N ratio for the sequences with the actual normalised S/N ratio. The sequences utilised in GRA are GRC. One of the two sequences that agrees with itself at every point is the value of GRC. The formulas to be used to calculate the GRC at the ith trial and the jth dependent variable response are shown in the relationship below.

$$GRC_{ij} = \frac{(\Delta_{min} + \lambda\Delta_{max})}{(\Delta_{ij} + \lambda\,\Delta_{max})} \qquad (7)$$

i=1, 2,3…..n, j=1,2,3…m response;

is the difference in absolute value between the reference sequence and comparability sequence, which is a divergence from the goal value and can be considered a quality loss.

Table9: Signal/Noise ratio values for the original response data (experimental results)

Ex.No.	Load (N)	SlidingSpeed (rpm)	Sliding Distance(mm)	Mass Loss	Co-eff
1	5	1	500	0.08	0.000808
2	5	1	750	0.23	0.001593
3	5	1	1000	0.23	0.001644
4	5	2	500	0.26	0.001711
5	5	2	750	0.27	0.0018
6	5	2	1000	0.3	0.002334
7	5	3	500	0.32	0.002902
8	5	3	750	0.33	0.003525
9	5	3	1000	0.35	0.003664

10	10	1	500	0.38	0.003965
11	10	1	750	0.39	0.004452
12	10	1	1000	0.39	0.004624
13	10	2	500	0.4	0.0048
14	10	2	750	0.42	0.006725
15	10	2	1000	0.44	0.007689
16	10	3	500	0.47	0.008789
17	10	3	750	0.5	0.008942
18	10	3	1000	0.51	0.012459
19	15	1	500	0.54	0.012561
20	15	1	750	0.56	0.013571
21	15	1	1000	0.6	0.014673
22	15	2	500	0.65	0.014695
23	15	2	750	0.65	0.016092
24	15	2	1000	0.65	0.017451
25	15	3	500	0.68	0.021057
26	15	3	750	0.73	0.02548
27	15	3	1000	0.74	0.028857

Table10: Normalized S/N ratio values
(output response data after data pre-processing)

Ex.No.	Norm ML	Norm CoF	Abs ML	Abs CoF
1	1	0.999992	-2.442E-15	8.149E-06
2	0.772727	0.972015	0.22727273	0.027984598
3	0.772727	0.970186	0.22727273	0.029814152
4	0.727273	0.967807	0.27272727	0.032193152
5	0.712121	0.964631	0.28787879	0.035369057
6	0.666667	0.94558	0.33333333	0.054419647
7	0.636364	0.925329	0.36363636	0.074671111
8	0.621212	0.90312	0.37878788	0.096880459
9	0.590909	0.898175	0.40909091	0.101824783
10	0.545455	0.887465	0.45454545	0.112535206
11	0.530303	0.870096	0.46969697	0.129903564
12	0.530303	0.863947	0.46969697	0.136052979
13	0.515152	0.857688	0.48484848	0.142312178
14	0.484848	0.789066	0.51515152	0.210934436
15	0.454545	0.754689	0.54545455	0.245311419
16	0.409091	0.71548	0.59090909	0.284519947

17	0.363636	0.710016	0.63636364	0.289983855
18	0.348485	0.584634	0.65151515	0.415365967
19	0.30303	0.580993	0.6969697	0.419006619
20	0.272727	0.54498	0.72727273	0.455020143
21	0.212121	0.505685	0.78787879	0.494314711
22	0.136364	0.504917	0.86363636	0.495083094
23	0.136364	0.455108	0.86363636	0.544892153
24	0.136364	0.406653	0.86363636	0.593347482
25	0.090909	0.278098	0.90909091	0.721902385
26	0.015152	0.120399	0.98484848	0.879601412
27	2.36E-15	-7.8E-06	1	1.000007843

Table11: Grey Relational Coefficient values and the Grey Relational Grade

GRC ML	GRC CoF	GRG
1	0.999984	0.999992
0.6875	0.946997	0.817249
0.6875	0.943727	0.815614
0.647059	0.939509	0.793284
0.634615	0.933935	0.784275
0.6	0.901844	0.750922
0.578947	0.870063	0.724505
0.568966	0.837689	0.703327
0.55	0.830807	0.690403
0.52381	0.81628	0.670045
0.515625	0.793772	0.654699
0.515625	0.786098	0.650862
0.507692	0.778438	0.643065
0.492537	0.7033	0.597919
0.478261	0.670861	0.574561
0.458333	0.637332	0.547833
0.44	0.632924	0.536462
0.434211	0.54623	0.49022
0.417722	0.544066	0.480894
0.407407	0.523549	0.465478
0.388235	0.502859	0.445547
0.366667	0.502471	0.434569
0.366667	0.478518	0.422592
0.366667	0.457311	0.411989
0.354839	0.409198	0.382018

0.336735	0.362424	0.349579
0.333333	0.333332	0.333332

The identifying or differentiating coefficients are the values of the Grey Relational Coefficient and the Grey Relational Grade. The range between 0 and 1 and the actual system requirements can be used to change the value. The value is used in this work as 0.5. Tables provide GRC values.

Step 4: The Grey Relational Grade (GRG) is produced using

Once after calculating GRC, it is a usual practice to collect the mean values of GRCs as GRG.

$$GRGi = 1/n \Sigma GRG_{ij} \quad (8)$$

nis the number of responses. The values are tabulated in table 4.6.

Table 12: ANOVA FOR MASS LOSS

Source	DF	Seq SS	Adj SS	MS	F	P
Load	1	0.653606	0.004789	0.004789	6.075	0.024663
SS	1	0.08405	0.002821	0.002821	3.578	0.075701
SD	1	0.010272	0.001873	0.001874	2.376	0.141585
L*L	1	0.002535	0.002535	0.002535	3.216	0.090738
SS*SS	1	0.000046	0.000046	4.63E-05	0.059	0.81142
SD*SD	1	0.000535	0.000535	0.000535	0.679	0.421385
L*SS	1	0.000008	0.000008	8.3E-06	0.011	0.919314
L*SD	1	0.000833	0.000833	0.000833	1.057	0.318292
SS*SD	1	0.000675	0.000675	0.000675	0.856	0.367747
Error	17	0.013402	0.013402	0.000788		
Total	26	0.765963				

Mass Loss = -0.260185 + 0.027 Load + 0.103611 SS + 0.000448889 SD +
0.000822222 L*L - 0.00277778 SS*SS - 1.51111e-007 SD*SD -
0.000166667 L*SS - 6.66667e-006 L*SD - 3e-005 SS*SD

S = 0.0280775 R-Sq = 98.25% R-Sq(adj) = 97.32%

R-Sq(pred) = 94.51%

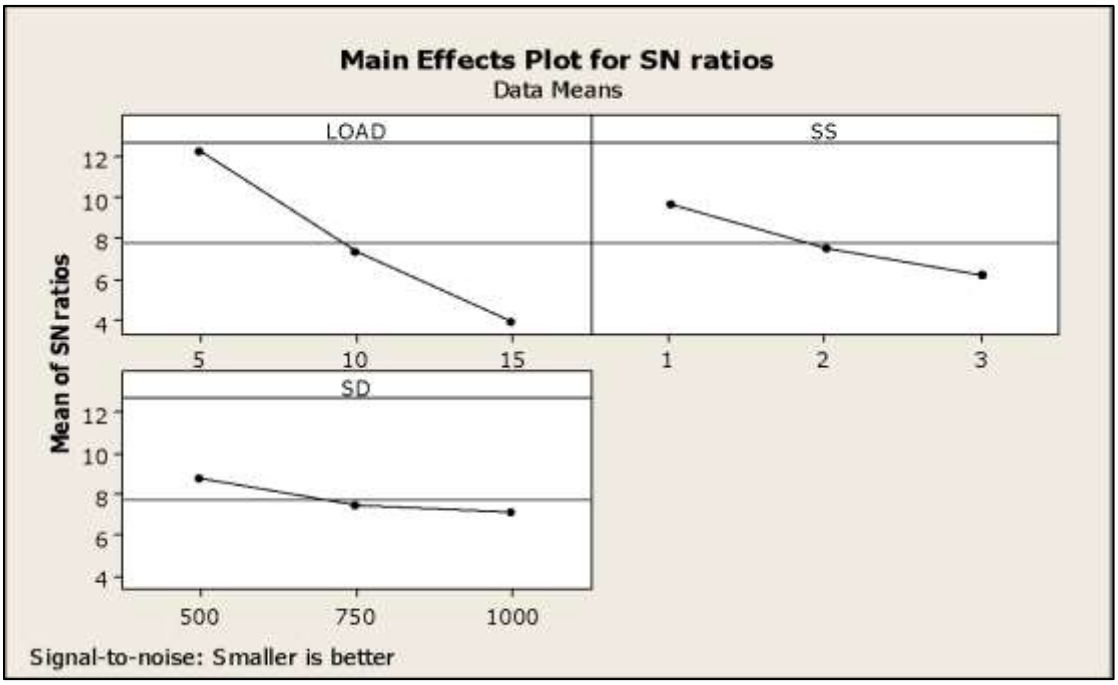

Figure 6:Signal to Noise Ratios (Mass loss)

From figure 6 it is observed that load of 10N, sliding speed of 750mm/sec and SOD of 2.2 mm gives optimal wear behaviour.

Table13: ANOVA FOR CoE

Source	DF	Seq SS	Adj SS	MS	F	P
Load	1	0.001159	4.15E-05	4.15E-05	36.723	0.000013
SS	1	0.000186	2.47E-05	2.47E-05	21.842	0.000218
SD	1	2.72E-05	6E-07	6E-07	0.557	0.4656
L*L	1	6.56E-05	6.56E-05	6.56E-05	58.017	0.000001
SS*SS	1	1.35E-05	1.35E-05	1.35E-05	11.91	0.003051
SD*SD	1	0	0	0	0.002	0.967417
L*SS	1	6.79E-05	6.79E-05	6.79E-05	60.011	0.000001
L*SD	1	9.1E-06	9.1E-06	9.1E-06	8.041	0.011415
SS*SD	1	6.2E-06	6.2E-06	6.2E-06	5.479	0.031697
Error	17	1.92E-05	1.92E-05	1.1E-06		
Total	26	0.001553				

Co-eff = 0.0182078 - 0.00251475 Load - 0.00969717 SS - 8.2338e-006 SD +

0.000132298 L*L + 0.00149855 SS*SS + 2.88006e-010 SD*SD +
0.000475711 L*SS + 6.96535e-007 L*SD + 2.87477e-006 SS*SD

S = 0.00106363 R-Sq = 98.76% R-Sq(adj) = 98.11%
R-Sq(pred) = 96.50%

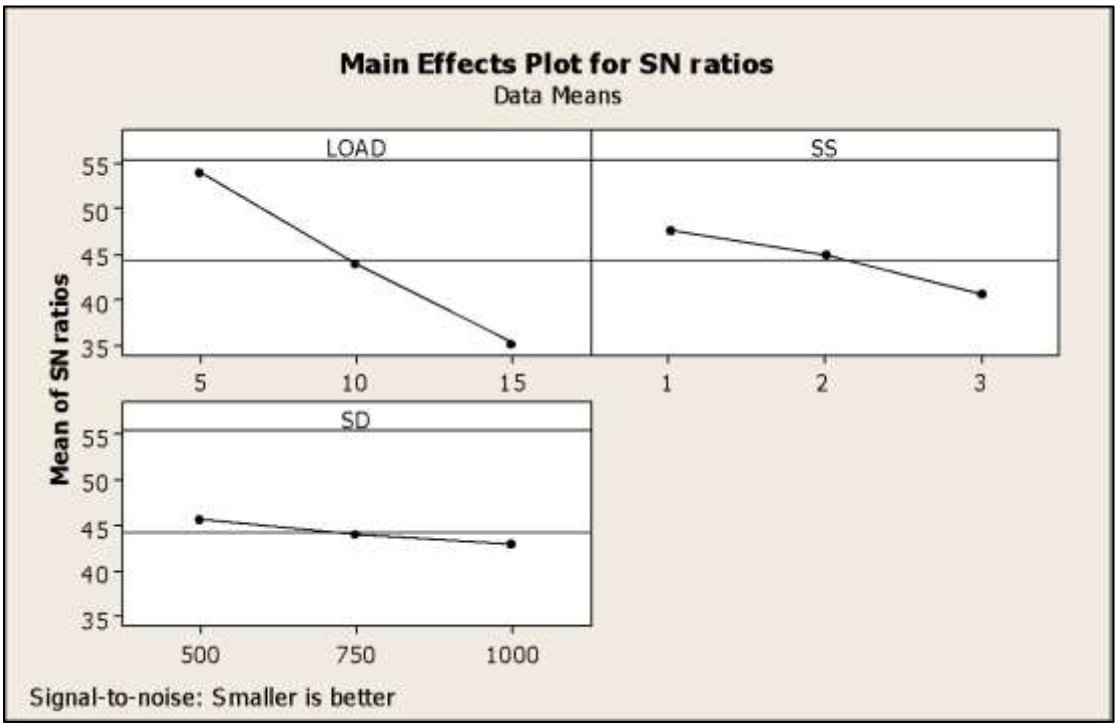

Figure7: Signal to Noise Ratios (Co-Efficient of Friction)

From figure 7 it is observed that load of 10 N, sliding speed of 750mm/sec and SOD of 2 mm gives optimal wear behaviour.

Conclusion

The PMMA + 5% B4C composites were successfully fabricated using the injection molding technique with the assistance of a single lead screw machine. The composites were then processed through abrasive water jet machining to prepare wear test samples, which were tested using a DUCOM instrument.

The wear test results revealed that the highest material removal rate was achieved at 160 MPa pressure, 3mm standoff distance, and 460mm/min transverse speed. Conversely, the lowest dimensional error was observed at 12 MPa pressure, 2mm standoff distance, and 460mm/min transverse speed. The optimal conditions for high material removal rate and minimal dimensional error were determined to be 160 MPa pressure, 3mm standoff distance, and 460 mm/min transverse speed, as established by the grey relational analysis technique.

In accordance with the results of the grey relational analysis, it was discovered that the mass loss and coefficient of friction were lowest at a 5N load, 1m/s sliding speed, and 500mm sliding distance. The incorporation of B4C nanoparticles demonstrated excellent wear resistance in the results. In the future, we plan to experiment with the addition of modified nanoparticles to the composite and examine their tribological properties.

Reference

1. Akinci ,S.Sen, U.Sen-Friction and wear behavior of zirconium oxide reinforced PMMA Composites : Part B 56 (2014) 42–47.

2. Fadhil K. Farhan, Bahjat B. Kadhim, Batool D. Ablawa and Warqaa A. Shakir-WearandFrictionCharacteristicsofTiO_2 –ZnO / PMMA Nanocomposites DOI: http://dx.doi.org/10.24018/ejers.2017.2.4.287 EJERS, European Journal of Engineering Research and Science Vol. 2, No. 4, April 2017

3. Li Zhenhua-The influence of silane surface treatment of SiO2 on the tribological property of PMMA composite filled with graphite. Journal of Thermoplastic Composite Materials 2014, Vol. 27(3) 297–305.
4. Zhenhua Li- The friction and wear properties of nano-SiO2 and -TiO2 particle-reinforced PMMA composites Journal of Thermoplastic Composite Materials 2014, Vol. 27(6) 793–800
5. Biswajit Saha a,b, Wei Quan Toh c, Erjia Liu d, Shu Beng Tor d,n, Junghoon Lee- A study on frictional behavior of PMMA against FDTS coated silicon as a function of load, velocity and temperature Tribology International 102 (2016) 44–51.
6. Feng-hua Sua, Zhao-zhu Zhang, Wei-min Liu a,-Friction and wear behavior of hybrid glass/PTFE fabric composite reinforced with surface modified nanometer ZnO Wear 265 (2008) 311–318.

7. Praveen Bhimaraj , David Burris , W. Gregory Sawyer , C. Gregory Toney , Richard W. Siegel , Linda S. Schadler- Tribological investigation of the effects of particle size, loading and crystallinity on poly(ethylene) terephthalate nanocomposites. Wear 264 (2008) 632–637.

8. Praveen Bhimaraj, David L. Burris, Jason Action, W. Gregory Sawyer, C. Gregory Toney, Richard W. Siegel, Linda S. Schadlera,- Effect of matrix morphology on the wear and friction behavior of alumina nanoparticle/poly(ethylene) terephthalate composites. Wear 258 (2005) 1437–1443.
9. Feng-hua Sua, Zhao-zhu Zhang, Wei-min Liu a,-Friction and wear behavior of hybrid glass/PTFE fabric composite reinforced with surface modified nanometer ZnO Wear 265 (2008) 311–318.

10. Praveen Bhimaraj , David Burris , W. Gregory Sawyer , C. Gregory Toney , Richard W. Siegel , Linda S. Schadler- Tribological investigation of the effects of particle size, loading and crystallinity on poly(ethylene) terephthalate nanocomposites. Wear 264 (2008) 632–637.

11. Praveen Bhimaraj, David L. Burris, Jason Action, W. Gregory Sawyer, C. Gregory Toney, Richard W. Siegel, Linda S. Schadlera,- Effect of matrix morphology on the wear and friction behavior of alumina nanoparticle/poly(ethylene) terephthalate composites. Wear 258 (2005) 1437–1443.

12. Yijun Shi, Xin Feng , Huaiyuan Wang, Xiaohua Lu- The effect of surface modification on the friction and wear behavior of carbon nanofiber-filled PTFE composites.
13. R.V. Kurahatti , A.O. Surendranathan , S. Srivastava, N. Singh, A.V. Ramesh Kumar, B. Suresha - Role of zirconia filler on friction and dry sliding wear behaviour of bismaleimide nanocomposites Materials and Design 32 (2011) 2644–2649.
14. Priyadarshi Tapas Ranjan Swaina , Sandhyarani Biswasa - Abrasive Wear Behaviour of Surface Modified Jute Fiber Reinforced Epoxy Composites Materials Research. 2017; 20(3): 661-674.
15. Priyadarshi Tapas Ranjan Swaina , Sandhyarani Biswasa - Abrasive Wear Behaviour of Surface Modified Jute Fiber Reinforced Epoxy Composites Materials Research. 2017; 20(3): 661-674.